TECHNICAL MEMORANDUM

X-471

PERFORMANCE AND CONTROL OF A FULL-SCALE, AXIALLY SYMMETRIC, EXTERNAL-INTERNAL-COMPRESSION INLET FROM MACH 2.0 TO 3.0

By David N. Bowditch, Bernhard H. Anderson, and William K. Tabata

Lewis Research Center
Cleveland, Ohio

NATIONAL AERONAUTICS AND SPACE ADMINISTRATION

WASHINGTON

May 1961

[redacted]

NATIONAL AERONAUTICS AND SPACE ADMINISTRATION

TECHNICAL MEMORANDUM X-471

PERFORMANCE AND CONTROL OF A FULL-SCALE, AXIALLY SYMMETRIC, EXTERNAL-INTERNAL-COMPRESSION INLET FROM MACH 2.0 to 3.0*

By David N. Bowditch, Bernhard H. Anderson,
and William K. Tabata

SUMMARY

A full-scale, axially symmetric inlet employing both external and internal supersonic compression was tested in conjunction with both an engine and a coldpipe in the 10- by 10-foot supersonic wind tunnel from Mach 2.0 to 3.0. Recovery reached 0.875 at a total bleed mass-flow ratio of 0.14 at Mach 2.88 and increased to 0.925 at Mach 2.00. Possible inlet control signals were investigated, and an electrical control system was used to position the centerbody by sensing an oblique shock originating at the cowl lip and to position the bypass by setting a constant throat-exit Mach number.

The effect of the streamwise position of an internal flow disturbance on the measured response of throat static pressure was investigated. The results are compared with a simple method of prediction.

INTRODUCTION

The capability of obtaining good internal performance with inlets employing internal supersonic compression at Mach numbers between 2.0 and 3.0 has been demonstrated with various designs, including those reported in references 1 to 3. However, to realize this high performance in an actual installation, an adequate control system must be provided. The control system must regulate the amount of internal contraction (by positioning the centerbody in the axisymmetric case) and must position the terminal shock near the peak recovery position by bypassing the correct amount of flow for inlet-engine matching. Some data pertaining to the control of axisymmetric internal-contraction inlets have been presented in references 4 and 5. Further, inlet-engine compatibility and

*Title, Unclassified.

[redacted]

inlet control operation of all-external-compression inlets have been investigated in both the 8- by 6-foot and 10- by 10-foot wind tunnels in the Mach 2.0 range (refs. 6 to 8). To extend this work in inlet-engine compatibility and control operation to inlets with internal compression and to a higher Mach number range, the inlet reported in reference 1 was scaled up to a 42-inch cowl-lip diameter and was tested with both an engine and a coldpipe at Mach numbers from 2.0 to 2.97 in the 10- by 10-foot tunnel. The inlet-engine compatibility information has been published in reference 9, and the present report presents the inlet performance and control information. This control investigation includes both centerbody or internal-contraction control and the bypass or terminal-shock control at Mach numbers from 2.00 to 2.97.

Inlet dynamics or the response of the control sensor to movement of the bypass has been previously investigated, and the results are presented in references 10 and 11. In reference 11, data are presented for control sensor response to oscillation of a bypass for coldpipe configurations of various volumes and lengths, and also for an engine configuration. The present report extends this work to cover oscillations or disturbances at three stations in a coldpipe configuration and two stations in an engine configuration. The lumped-parameter method for prediction of inlet dynamics presented in reference 11 is compared with the data.

SYMBOLS

A	flow area, sq ft
A_c	inlet-capture area, 9.62 sq ft
D_c	cowl-lip diameter, 42 in.
M_0	free-stream Mach number
m_b	bypass mass flow, slugs/sec
m_t	throat bleed mass-flow, total flow removed through both cowl and centerbody flush slots at the throat, slugs/sec
m_0	inlet-capture mass flow, slugs/sec
m_2	mass flow at engine-face station, slugs/sec
m^*	choking mass flow based on cowl-lip annular area and free-stream conditions, slugs/sec
$P_{b,ref}$	bypass-control reference pressure, lb/sq ft

P_{cb}	centerbody-control sensor pressure, lb/sq ft
$P_{cb,ref}$	centerbody-control reference pressure, lb/sq ft
P_0	free-stream total pressure, lb/sq ft
$\bar{P}_2$	average total pressure at engine-face station, lb/sq ft
ΔP_2	maximum total pressure minus minimum total pressure at engine-face station, lb/sq ft
$\bar{P}_{2r}$	average total pressure at constant radius, lb/sq ft
p	static pressure, lb/sq ft
p_b	bypass-control sensor pressure, lb/sq ft
R	radial distance from model centerline to cowl inner surface, in.
r	radial distance from model centerline, in.
w	weight flow, lb/sec
$(w\sqrt{\theta/\delta})_2$	corrected weight flow at engine face, lb/sec
x	downstream distance from cowl lip, in.
δ	ratio of total pressure to NASA standard sea-level pressure of 2116 lb/sq ft
θ	ratio of total temperature to NASA standard sea-level temperature of 518.7° R
θ_l	centerbody position parameter (angle between model centerline and line connecting spike tip and cowl lip), deg

APPARATUS AND PROCEDURE

An external-internal-compression inlet was tested in the 10- by 10-foot supersonic wind tunnel in combination with both an engine and a coldpipe. Several Mach numbers from 2.00 to 2.97 and angles of attack from 0° to 5° were investigated at a Reynolds number of 2.0×10^6 per foot.

Figure 1 shows the inlet installed in the 10- by 10-foot wind tunnel. The inlet was aerodynamically similar to the inlet reported in reference 1

but was scaled up to a 42-inch cowl-lip diameter. External compression was obtained in the flow field of a 20° half-angle conical centerbody. Internal supersonic compression was obtained in the flow field generated by the cowl, which turned the flow 12° axially inward at both the cowl lip and at an internal step. At a Mach number of 2.88, the inlet operated as designed with the two internal oblique shocks coalescing at the centerbody shoulder.

A cutaway view of the inlet showing the main and vernier bypass valves, the bleed system, and the internal flow passages is presented in figure 2. An annular bypass just ahead of the engine face matched the engine and inlet airflows. The cowl inner wall diverged just ahead of a bellmouth to allow air to flow annularly around the engine or coldpipe. The flow was regulated by choking the passage between the engine bellmouth and the annular bypass valve, which could be translated axially by three hydraulic cylinders or oscillated for duct dynamic investigations. A vernier bypass just upstream of the centerbody struts was used to introduce flow disturbances near the terminal shock for a duct dynamics investigation. The flow left the duct through a slot in the cowl inner wall, and the disturbances were introduced by circumferentially oscillating the vernier bypass valve to vary the choked flow area between the valve holes and the fixed holes in the inner cowl structure. The centerbody was translated axially by a hydraulic cylinder to vary the inlet contraction.

Flush bleed slots can be seen in figure 2 on the centerbody shoulder and downstream in the throat. Shoulder bleed slot "a" removed the boundary layer at the point of impingement of the oblique shocks from the cowl. Throat bleed slots "b" and "c" removed the boundary layer in the terminal-shock region and were placed so they were opposite each other at the optimum centerbody position at Mach 2.88. These bleeds were designed to remove 0.4 of the bleed in this region through the centerbody slot and 0.6 through the cowl slot. The inlet was investigated without this downstream bleed and with two sizes of downstream bleed slots. The detail dimensions of the shoulder bleed slot are presented in figure 3(a), and the cowl and centerbody bleed-slot dimensions are presented in figures 3(b) and (c), respectively.

The inlet area distribution to the engine face is presented in figure 4. The area distribution is shown for four centerbody positions from near maximum contraction (θ_l = 29.80°) to the position of maximum throat area (θ_l = 26.75°), where the centerbody shoulder is opposite the cowl step.

The inlet-engine and inlet-coldpipe configurations are shown in figure 5. The centerbody static-pressure distributions were obtained

from a line of statics on the horizontal centerline. Six 7-tube rakes, located at the engine face (station 2), were used to obtain inlet recovery and flow distortion. The coldpipe-configuration mass flows were calculated by using statics in the coldpipe and assuming that the plug exit area was choked. Bleed flows were then obtained by subtracting this flow from the estimated flow entering the inlet at the cowl lip (station 1). This entering flow was estimated from the known conditions in the flow field of a 20° half-angle cone (ref. 12). The mass flows and corrected weight flows at subsonic speeds were obtained from the measured speed-flow characteristics of the engine and from the recovery, which was measured by two 7-tube rakes (duplicates of two of the six coldpipe rakes) at the engine face (station 2).

One of the objectives of the test was to find the effect of disturbance location on the inlet dynamics; accordingly, sinusoidal disturbances were introduced by the vernier bypass, the main bypass, and the mass-flow control plug. Phase shift of the bypass pressure sensor p_b and the amplitude ratio of the bypass static pressure were measured from traces of sinusoidal oscillation of the plug or bypass and from the response of p_b and the bypass static. These traces were obtained with an optical oscillograph.

To illustrate the usefulness of possible inlet control sensor pressures, the electrical inlet control system shown schematically in figure 6 was investigated. The centerbody control used a sensor that measured the Pitot pressure rise associated with the oblique shock impinging on the shoulder, and the bypass control sensed the static-pressure variation just downstream of the centerbody bleed slot. The control sensor and reference pressures were sensed by transducers whose output voltage was proportional to the absolute pressure measured. To set the desired control ratio, a fraction of the reference pressure voltage, equal to the desired ratio, was compared with the entire sensor voltage by the circuit in the control ratio box. The difference between the voltages in this comparison is the error signal. This error signal was then fed into the servoamplifier, which opened the hydraulic valve to obtain movement of the bypass or centerbody in the proper direction.

RESULTS AND DISCUSSION

Inlet Performance

The peak inlet performance is presented in figure 7 for 0, 0.06, and about 0.12 throat bleed mass-flow ratios (an additional 2 counts of centerbody shoulder bleed was required to keep the inlet started with the centerbody in the design position). For all bleed flows, the recovery remained high throughout the range from Mach 2.0 to 2.88 but

declined rapidly between Mach 2.88 and 2.97, probably because the internal compression was operating aerodynamically above its design Mach number. The maximum recovery was 0.875 with a total (throat plus shoulder) bleed of 0.14 at Mach 2.88 and increased to 0.925 at Mach 2.00. Bleeding about 6 and 13 percent of the capture mass flow at the throat increased the recovery only about 2 and 4 percent, respectively, which indicated the ineffectiveness of the particular bleed system investigated. The performance with the inlet unstarted, but with the mass-flow control plug and centerbody in the same position as for peak recovery, is shown for comparison. At Mach numbers of 2.49 and below, the subcritical pressure recovery was only about 5 counts lower than the peak value; but, at Mach 2.88, the recovery dropped 30 counts with a similar mass-flow reduction. Since this happens almost instantaneously, it represents a very severe transient, which would probably cause engine surge, as was shown in reference 10.

The inlet distortion with no bleed was quite high ($\approx$0.20) over the range of Mach numbers investigated. However, except at the highest Mach number, the distortion was reduced about 5 counts for each 6 counts additional bleed, so that the bleed effectively reduced the distortion even though it had little effect on recovery. Total-pressure distributions are presented in figure 8 to illustrate the type of distortions obtained as the bleed flow is varied. The average radial distribution is presented because there was little circumferential distortion at these conditions. At Mach 2.88 and no throat bleed (squares), there were low-pressure regions at both the cowl and centerbody. Bleed counts of 6 and 12 successively improved the distortion profiles with greater improvement at the cowl surface than at the centerbody. The poor centerbody flow was even more prominent at Mach 2.97 and about 0.12 bleed mass-flow ratio. This is because the two cowl shocks coalesced before they reached the centerbody, causing a low recovery region at the centerbody.

The peak inlet performance with a throat bleed mass-flow ratio of 0.06 is presented in figure 9. For peak performance, the flow control plug was closed to the smallest area that could be set without unstarting the inlet. At high Mach numbers the recovery increased rapidly as the spike position angle θ_l was increased, and reached a peak at or near the highest θ_l or maximum contraction at which the inlet remained started. The inlet performance at Mach numbers near 3.0 was quite sensitive to angle of attack. For example, at Mach 2.88, increasing the angle of attack from 0° to 2.5° reduced the maximum started spike position angle 1.14° with a resultant loss in recovery of over 11 counts. It is interesting to note that the loss in recovery appears to be due to the reduction in maximum θ_l for a started inlet, as the recovery at the same spike position remained almost constant to angles of attack from 0° to 5° at Mach 2.88. The recovery and distortion were less dependent on spike position and angle of attack at Mach numbers near 2; this is partially due to the reduction of the internal compression and to the fact that the internal oblique shocks were weak or no longer existed.

The radial distortion with a low-energy region near the centerbody caused a problem when large amounts of flow were bypassed, as might happen during inlet restarting. Figure 10(a) illustrates the effect of bypassing progressively larger amounts of flow on the average radial pressure distribution. It can be seen that, when large amounts of flow are bypassed, most of the high recovery air leaves the duct with the result that a large separated region forms around the centerbody. Figure 10(b) shows that relatively large amounts of mass flow can be bypassed with only small losses in recovery; however, the main problem is the large separated region that can adversely affect engine operation.

Inlet operation at approximately Mach 0.10 is presented in figure 11. Figure 11(a) shows the recovery plotted against a parameter m_2/m^* used in reference 13, in which recovery of sharp-lip inlets at low speed is analyzed. The parameter m_2/m^* is the ratio of the engine-face mass flow divided by the mass flow that could pass through the annular area at the cowl lip, so that m^* is a function of centerbody position θ_l, which determines the annular cowl-lip area. The limits were obtained from reference 13 for zero velocity conditions and are determined by choking between the centerbody shoulder and cowl step and between the shoulder and cowl lip at θ_l of 26.75° and 23.90°, respectively. The minumum and maximum values of m_2/m^* correspond to corrected weight flows of about 97 and 152 pounds per second at both centerbody positions. Therefore, the corrected weight flow at a value of m_2/m^* is much higher at $\theta_l = 26.75^\circ$ than at $\theta_l = 23.90^\circ$. According to reference 13, the recoveries should be independent of configuration (centerbody position in this case) and a function of m_2/m^* only, except near choking conditions when the inlet has internal contraction. The recoveries at both centerbody positions are quite similar, and the difference in recovery between the two centerbody positions at m_2/m^* of 0.62 is caused by losses due to the approach of choking conditions at the throat with $\theta_l = 26.75^\circ$ (choking occurs near $m_2/m^* = 0.68$, as indicated by limit). Opening the cowl bleed and allowing flow to enter through the bleed system dropped the recovery about 1 count. No attempt was made to compare the predicted and actual recoveries, because the predicted value is very dependent on the unknown far-field Mach number. Only the measured tunnel Mach number, which is in the flow field affected by the engine in the restricted test section, was known. Figure 11(b) shows that the distortion was the same for both centerbody positions and was a function of only the engine corrected weight flow.

[redacted]

Centerbody Position Control

In order to obtain the peak performance from an internal-contraction inlet, both the internal contraction - or centerbody position in this case - and the terminal-shock or bypass positions must be continuously positioned to their optimum values. In order to investigate possible control signals, the electronic controls described in the section APPARATUS AND PROCEDURE were investigated.

The inlet was designed so the oblique shock from the cowl lip would fall on the centerbody shoulder at Mach numbers from 2.00 to 2.97. Therefore, it was possible to sense the shock pressure rise at the shoulder and use it to position the centerbody. This was done by a total-pressure tube P_{cb} embedded in the lip of the centerbody shoulder bleed slot. A ratio of this total pressure to a total located behind the cowl lip $P_{cb,ref}$ (fig. 6) was set by the control, and the resulting centerbody positions are presented in figure 12. The highest ratio shown for each Mach number is the maximum value that would not cause shock regurgitation. The ratios are less than 1 because of boundary layer and the local expansion due to the upstream surface of the shoulder bleed. The control was able to set the optimum centerbody position at all Mach numbers, and at most conditions the centerbody was set at or near the optimum value over a range of 0.10 in the ratio. The notable exception is at Mach 2.68, where the throat evidently became too small before the full shock pressure rise was felt on the shoulder. However, it appears that the centerbody can be positioned very well by scheduling a ratio with free-stream Mach number for the closed-loop spike control.

Bypass Control

To investigate bypass controls, it is of interest to investigate first the pressure distributions in the throat to find a usable control pressure signal. Figure 13 presents the change in centerbody static-pressure distributions in the throat region with recovery at Mach 2.88 and 2.49. At Mach 2.88, (fig. 13(a)), the terminal shock reached the centerbody slot at a recovery of 0.822, which was the maximum recovery with no throat bleed. The shock then remained on the slot until a recovery of 0.851 was reached. Finally, at a peak recovery of 0.854 the shock moved ahead of the slot and appeared to furnish an excellent control signal ahead of the slot. However, this signal was not consistent throughout the inlet operating range. For example, at Mach 2.48 (fig. 13(b)), when the centerbody slot had been translated ahead of the cowl bleed slot to decrease inlet contraction, the terminal shock never moved ahead of the slot as it did at Mach 2.88. It therefore appears, from analysis of the remainder of the data and from consideration of additional requirements such as a decrement in recovery for inlet stability, that

[redacted]

it is not feasible to find one station where a major part of the terminal shock pressure rise can be measured at all conditions to set peak recovery.

The static pressures just downstream of the slot appear to furnish a rather attractive control signal, since they varied consistently with recovery, although they did not furnish a signal of large amplitude or gain. Figure 14 presents the steady-state performance, at 0° angle of attack, for a control using the static pressure just downstream of the spike slot (labeled "sensor" in fig. 13) as a sensor and a reference total in the throat $P_{b,ref}$ (fig. 6). After a survey of the available reference pressures, the throat total was chosen because it kept the control pressure ratio at peak recovery almost constant. A constant control pressure ratio of 0.74 set peak recovery at Mach numbers from 2.28 to 2.68 and set recovery within 2 percent of the peak at Mach numbers of 2.00 and 2.88. Setting a constant ratio of throat static to throat total pressure is equivalent to setting a constant Mach number at the downstream edge of the slot. Setting a constant throat-exit Mach number to obtain peak recovery appears to have general application, as the same parameter was found to be usable for a Mach 3.0, two-dimensional inlet with porous bleed. In that inlet, as with the inlet of this report, it was not feasible to sense the full shock pressure rise because the peak recovery shock station varied with inlet condition and did not coincide with the geometric throat station. It therefore appears that the bypass control will have to use a control sensor location similar to that presented in figure 14, which has a much smaller gain than is usually associated with sensing a terminal shock pressure rise.

Inlet Dynamics

In predicting the dynamic performance of the bypass control, the response of the control pressures in the inlet throat to bypass movement is of primary importance. These inlet-turbojet dynamics were initially discussed in reference 10. Reference 11 presents the results of an investigation that explored the effect of coldpipe volume and of an engine on the measured response. A simple prediction of the measured dynamics was also presented in reference 11; this prediction consisted of a dead time based on the acoustic travel time from the bypass to the throat in series with a lumped-parameter, first-order system based on the capacitance of the diffuser and engine or coldpipe volumes. Since the two systems were considered to be in series, the assumed sequence of events following an increase in the bypass area was: (1) a change in the pressure in the diffuser-coldpipe volume as defined by the lumped-parameter first-order system, and (2) transmission of this pressure change by

acoustic waves to the throat with no change in amplitude but with an elapsed time equal to the dead time. Because this sequence went from the bypass to the diffuser and then to the throat, it appeared that the streamwise location of the disturbance, and particularly locating the disturbance at the throat, might have some effect on the accuracy of prediction. Therefore, flow disturbances were introduced near the throat, at the diffuser exit for both the coldpipe and engine configurations, and at the exit for the coldpipe configuration only.

The phase shift of the static-pressure sensor p_b just downstream of the bleed slots to disturbances generated at three duct locations is presented in figure 15. The amplitude ratio presented was obtained from the bypass static, because the pressure variation at p_b was too nonlinear to permit data reduction, and theory predicts constant amplitude ratio throughout the duct. The scatter in the data is caused by the nonlinear pressure response to bypass movement, and the noise is due to the terminal shock. The amplitude-ratio data in figure 15(a) do not show any resonance, which is compatible with the first-order prediction. Since the dead-time system is assumed to transmit the signal at a constant amplitude, the predicted amplitude-ratio decrease is due to the first-order system only. The predicted curve, which is based on the sum of the diffuser volume (42.8 cu ft) and the coldpipe volume (72.5 cu ft), fits the data fairly well. Even the response to oscillation of the vernier bypass, which was only inches downstream of the throat, appears to follow the predicted first-order system, although it did have the highest amplitude of the three disturbances.

The predicted phase shift (fig. 15(b)) for the plug oscillation, which is made up of the phase shift due to both the first-order system and the dead time, is as much as 40 percent too high in the intermediate frequencies of 2 and 3 cycles per second. However, the agreement improves as frequency increases, so that the prediction is only about 15 percent above the measured values at 8 and 10 cycles per second. The vernier and main bypass data are very similar, and the data scatter obscures the dead-time difference of about 0.005 second. Most of the vernier and main bypass phase-shift data fall above the first-order curve; and the predicted phase shift for the vernier bypass, for which the dead-time phase shift is negligible, fits the data best. Therefore, the prediction appears to be at least as accurate for disturbances near the shock as for disturbances downstream in the plenum, on whose volume the first-order system is based.

The response of p_b to vernier and main bypass disturbances in an engine-inlet configuration is shown in figure 16. The predicted amplitude ratio appears to be about the best single curve that could be drawn through the scattered data. The first-order system, which is based on the sum of the diffuser volume of 42.8 square feet and the corrected engine volume of 10.6 cubic feet, fits the phase-shift data the best at

the frequencies measured. The corrected engine volume is based on a constant ΔP throughout the engine, because this assumption was empirically shown to be best in reference 11. In this case, however, the correction effect was small, since the uncorrected engine volume was about 12.7 cubic feet and the difference of 2.1 cubic feet causes only about a 4-percent change in the total diffuser plus engine volume.

SUMMARY OF RESULTS

A large, 42-inch cowl-lip diameter, axially symmetric inlet employing both external and internal supersonic compression was tested in conjunction with both an engine and a coldpipe in the 10- by 10-foot supersonic wind tunnel. Inlet performance, control, and dynamics were investigated with the following results.

1. The throat bleed system investigated in this inlet was very effective in reducing distortion but was of questionable value for improving recovery.

2. When large amounts of flow were bypassed annularly ahead of the engine face, the high recovery air tended to go out the bypass with the result that a large separated region formed around the centerbody.

3. The inlet was designed so that the internal oblique shock from the cowl lip fell on the centerbody shoulder from Mach 2.0 to 3.0, and it was found experimentally that sensing this shock pressure rise on the shoulder provided an adequate centerbody position control signal.

4. Because the peak recovery shock station varied with inlet conditions such as contraction and free-stream Mach number, it was not possible to sense the full terminal shock pressure rise at a single station for bypass control.

5. Setting a constant Mach number just downstream of the throat (which was found in previous work to be an attractive bypass control parameter for the two-dimensional inlet) appeared to be a very useful parameter for controlling bypass position.

6. The streamwise location of an internal disturbance had little effect on the accuracy of a simple prediction method (a lumped-parameter, first-order system based on diffuser capacity to store mass, in series with an acoustic dead time) when used to predict the response of static pressures in the throat to the choked exit area disturbances.

Lewis Research Center
National Aeronautics and Space Administration
Cleveland, Ohio, January 27, 1961

REFERENCES

1. Obery, Leonard J., and Stitt, Leonard E.: Performance of External-Internal Compression Inlet with Abrupt Internal Turning at Mach Numbers 3.0 to 2.0. NACA RM E57H07a, 1957.

2. Stitt, Leonard E., and Salmi, Reino J.: Performance of a Mach 3.0 External-Internal-Compression Axisymmetric Inlet at Mach Numbers from 2.0 to 3.5. NASA TM X-145, 1960.

3. Bowditch, David N., and Anderson, Bernhard H.: Performance of an Isentropic, All-Internal-Contraction, Axisymmetric Inlet Designed for Mach 2.50. NACA RM E58E16, 1958.

4. Anderson, Bernhard H., and Bowditch, David N.: Performance of Three Isentropic All-Internal-Compression Axisymmetric Inlets Designed for Mach 2.5. NASA TM X-259, 1960.

5. Anderson, Bernhard H., and Bowditch, David N.: Investigation of Inlet Control Parameters for an External-Internal-Compression Inlet from Mach 2.1 to 3.0. NACA RM E58G08, 1958.

6. Wilcox, Fred A.: Investigation of a Continuous Normal-Shock Positioning Control of the Bypass of a Supersonic Inlet in Combination with the J34 Turbojet Engine. NACA RM E55J10, 1956.

7. Wilcox, Fred A.: Investigation of a Continuous Normal-Shock Positioning Control for a Translating-Spike Supersonic Inlet in Combination with J34 Turbojet Engine. NACA RM E57G16, 1957.

8. Hearth, Donald P., and Anderson, Bernhard H.: Use of Constant Diffuser Mach Number as a Control Parameter for Variable-Geometry Inlets at Mach Number of 1.8 to 2.0. NACA RM E57G02, 1957.

9. Bowditch, David N., Anderson, Bernhard H., and Tabata, William K.: Performance of a Turbojet Engine in Combination with an External-Internal-Compression Inlet to Mach 2.88. NASA TM X-254, 1960.

10. Wilcox, Fred, and Whalen, Paul: Dynamics of a Supersonic Inlet with Adjustable Bypass in Combination with a J34 Turbojet Engine. NACA RM E55L13a, 1956.

11. Bowditch, David N., and Wilcox, Fred A.: Dynamic Response of a Supersonic Diffuser to Bypass and Spike Oscillation. NASA TM X-10, 1959.

12. Anon.: Tables of Supersonic Flow Around Cones. Rep. No. 1, Dept. Elec. Eng., M.I.T., 1947.

13. Fradenburgh, Evan A., and Wyatt, DeMarquis D.: Theoretical Performance Characteristics of Sharp-Lip Inlets at Subsonic Speeds. NACA Rep. 1193, 1954. (Supersedes NACA TN 3004.)

E-1092

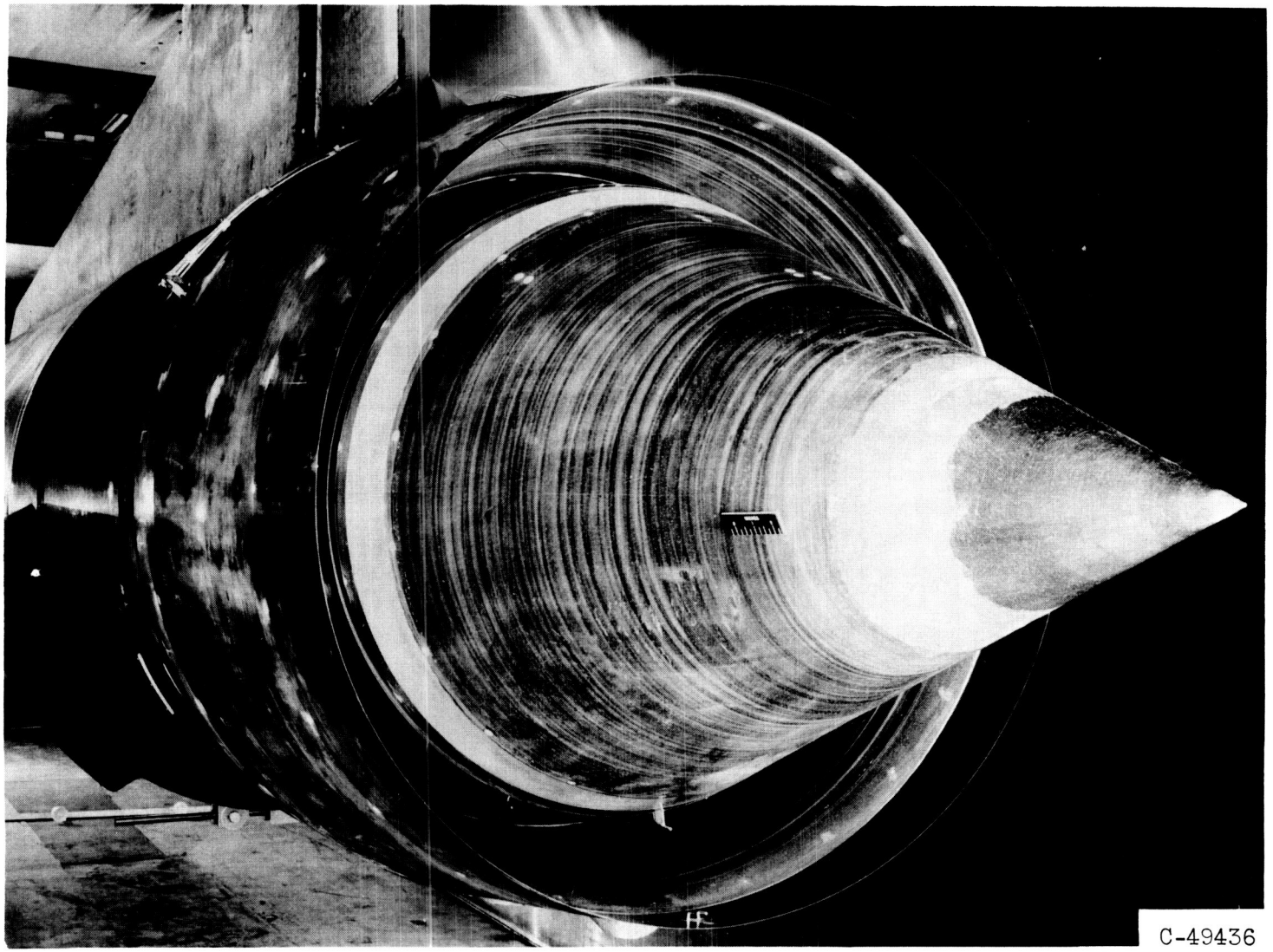

Figure 1. - External-internal-compression supersonic inlet installed in 10- by 10-foot wind tunnel.

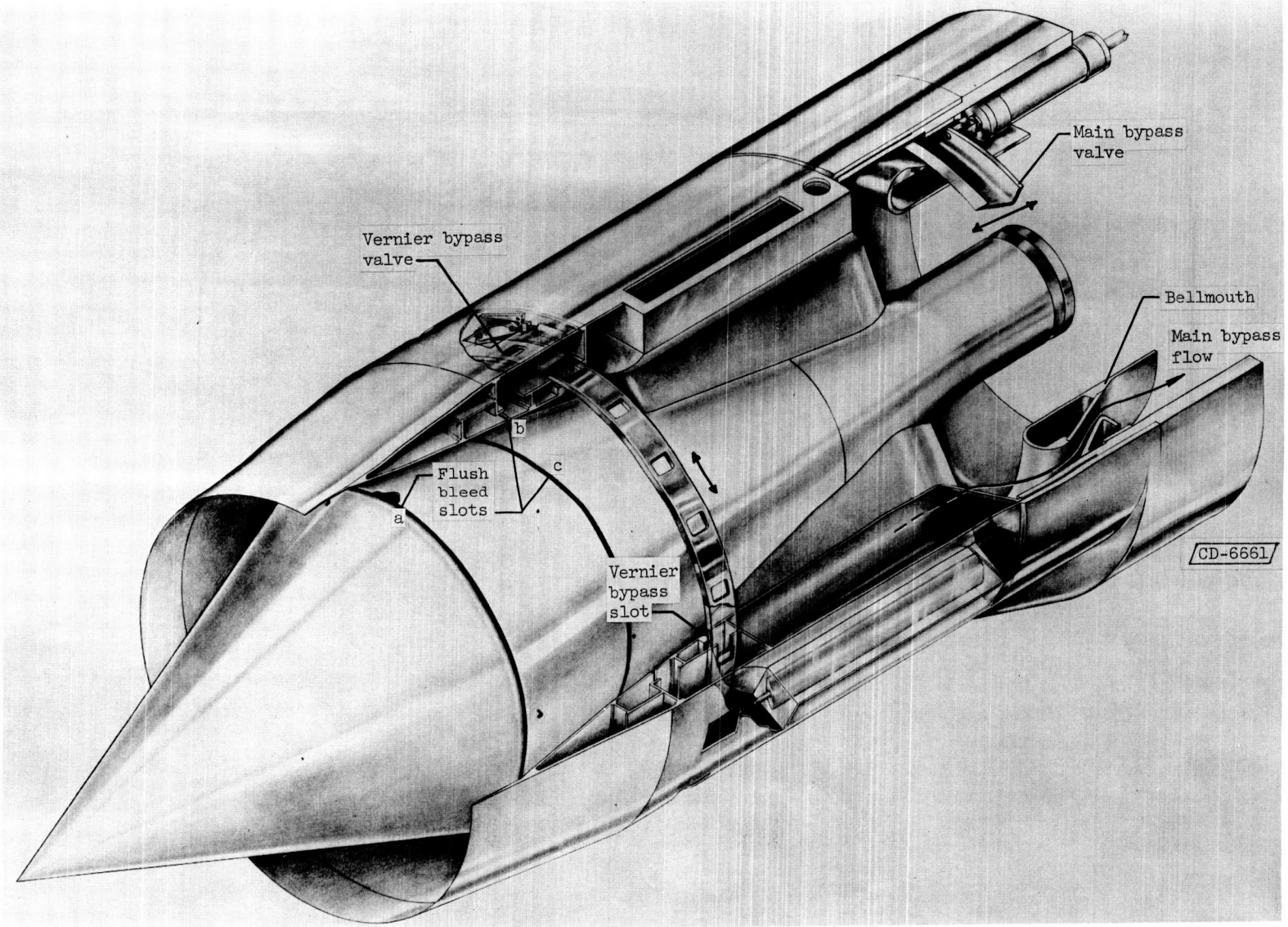

Figure 2. - Cutaway view of inlet.

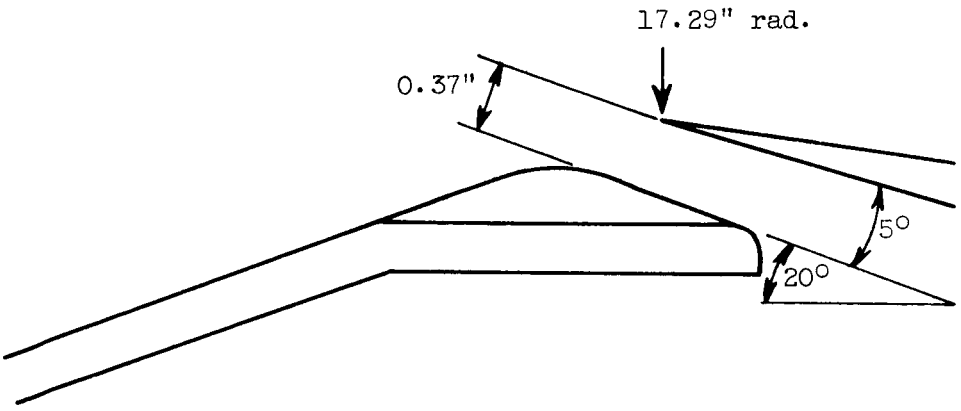

(a) Shoulder bleed slot.

Figure 3. - Bleed-slot configurations.

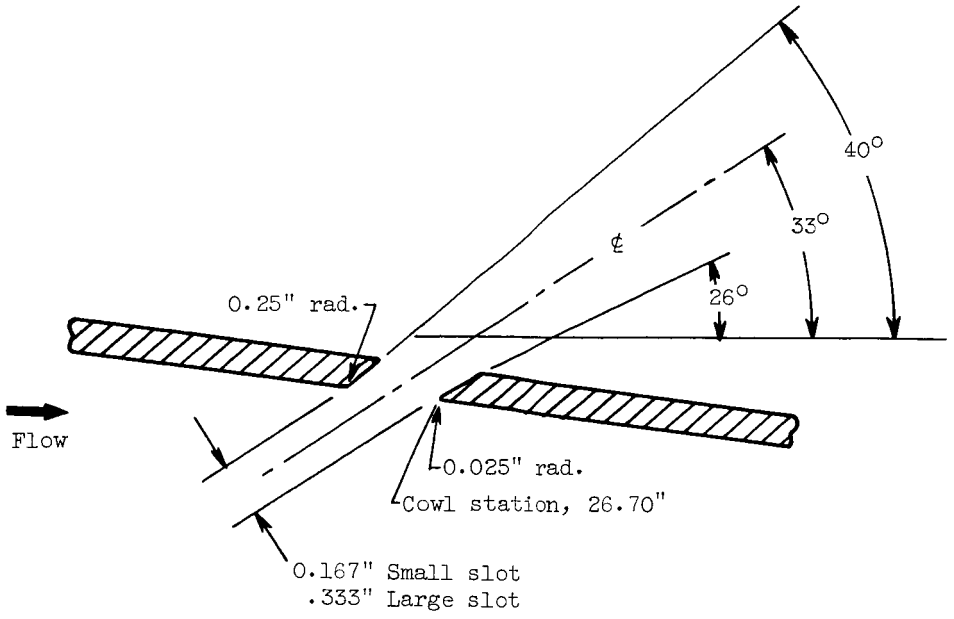

(b) Cowl bleed slot.

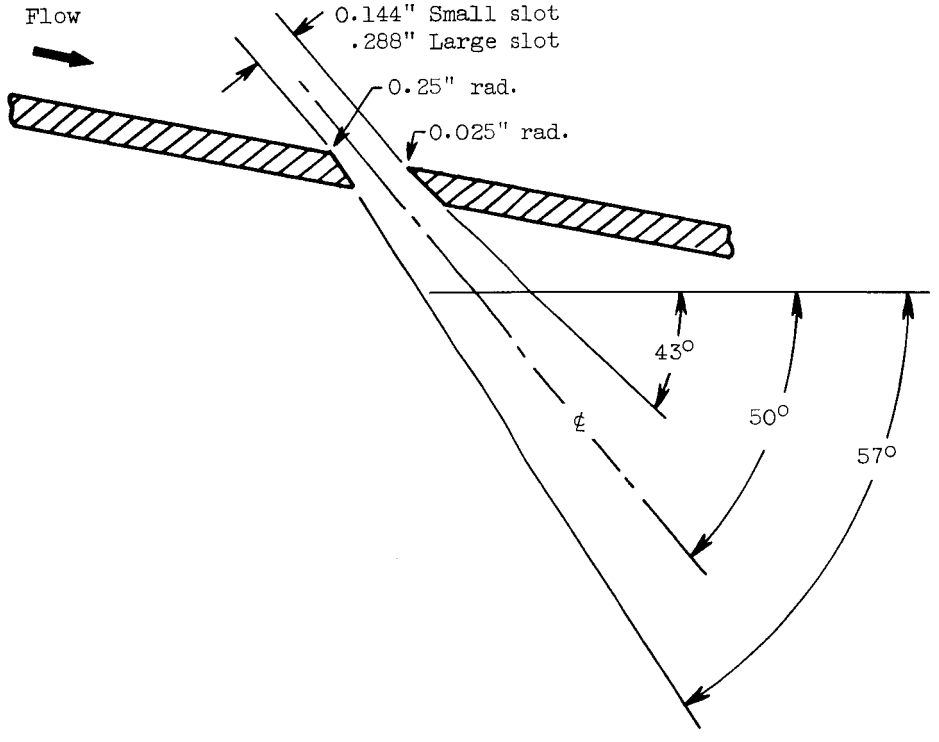

(c) Centerbody bleed slot.

Figure 3. - Concluded. Bleed-slot configurations.

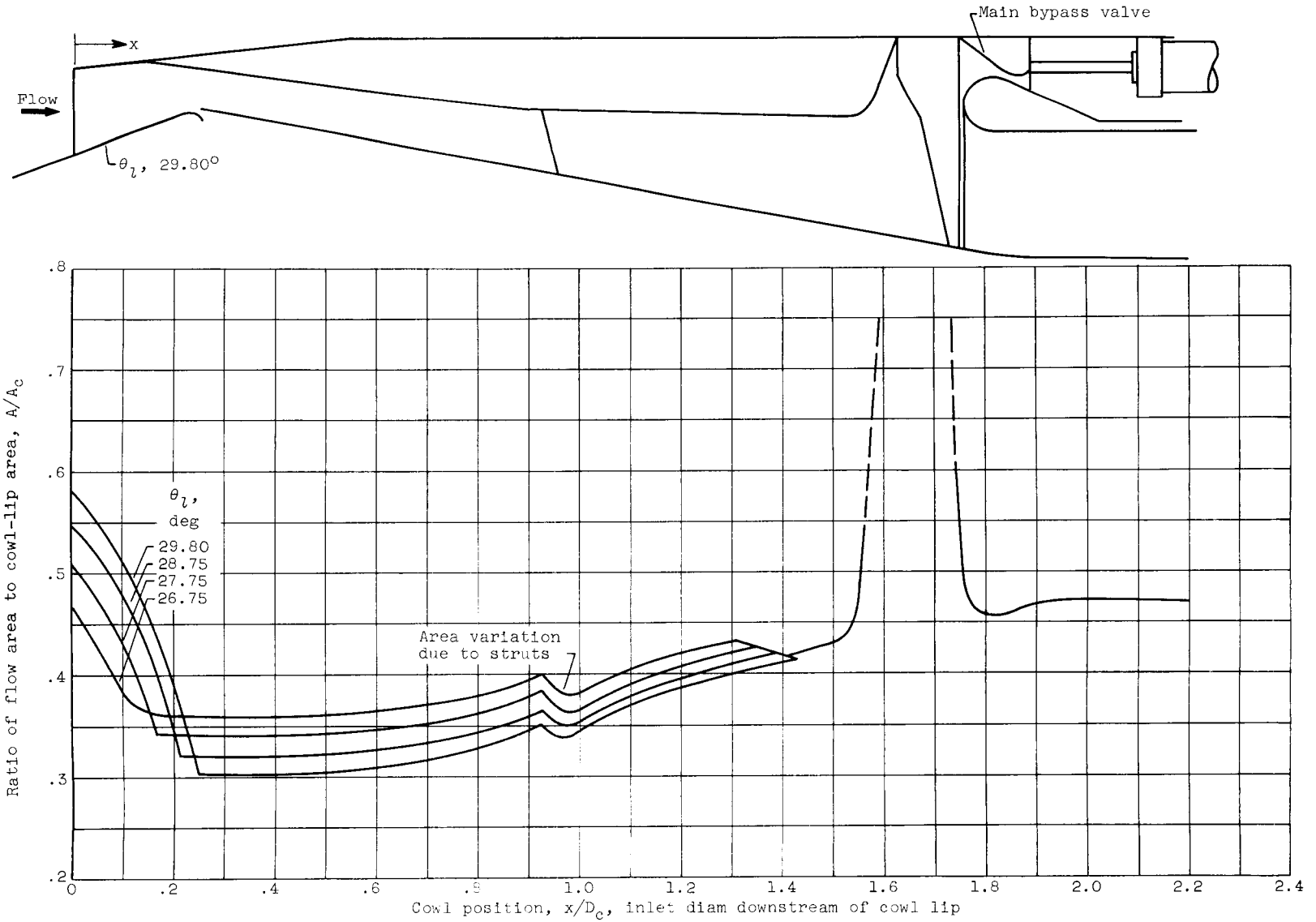

Figure 4. - Inlet area distribution.

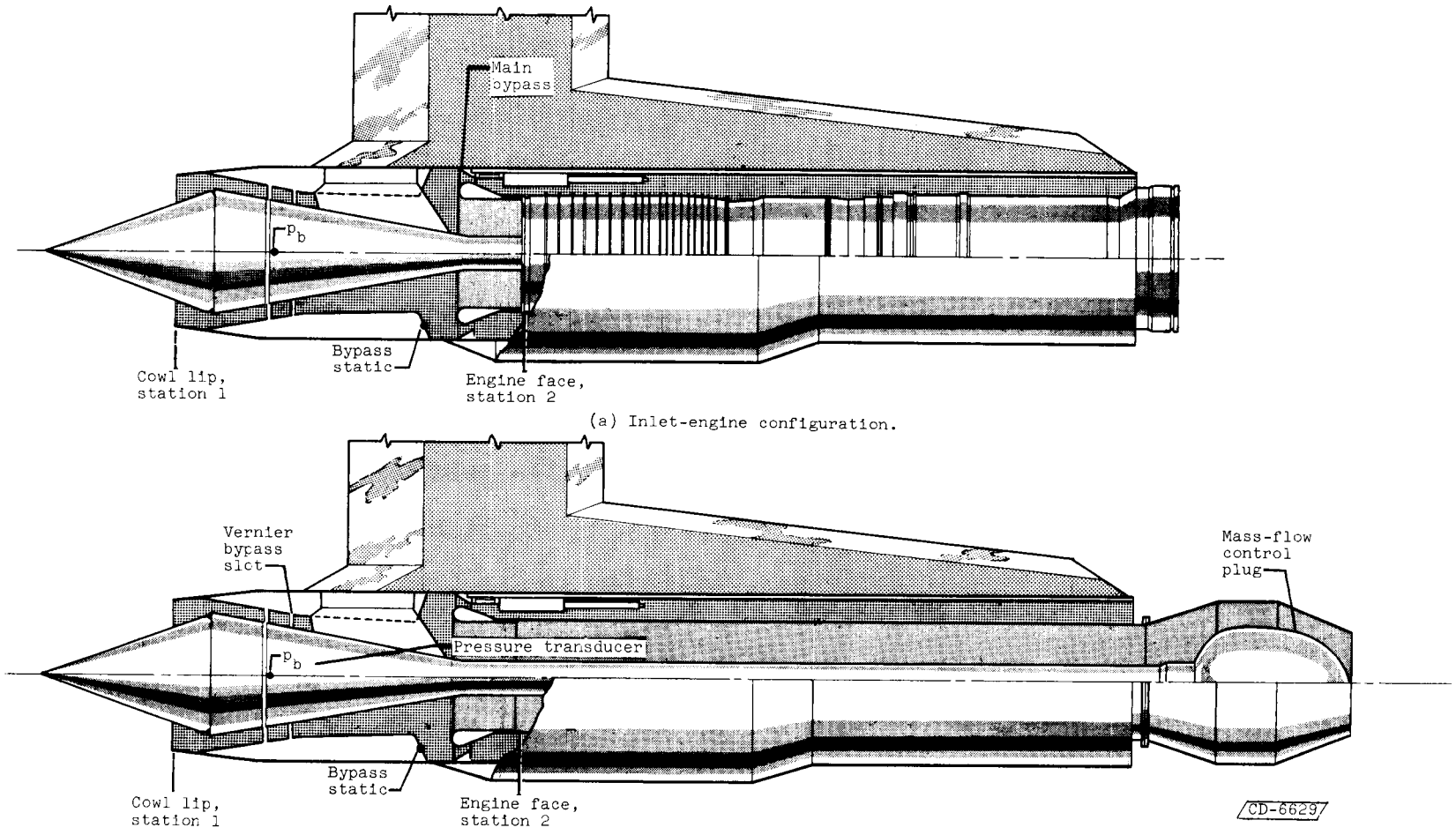

(a) Inlet-engine configuration.

(b) Coldpipe configuration.

Figure 5. - Cutaway view of nacelle showing installation of turbojet engine and coldpipe.

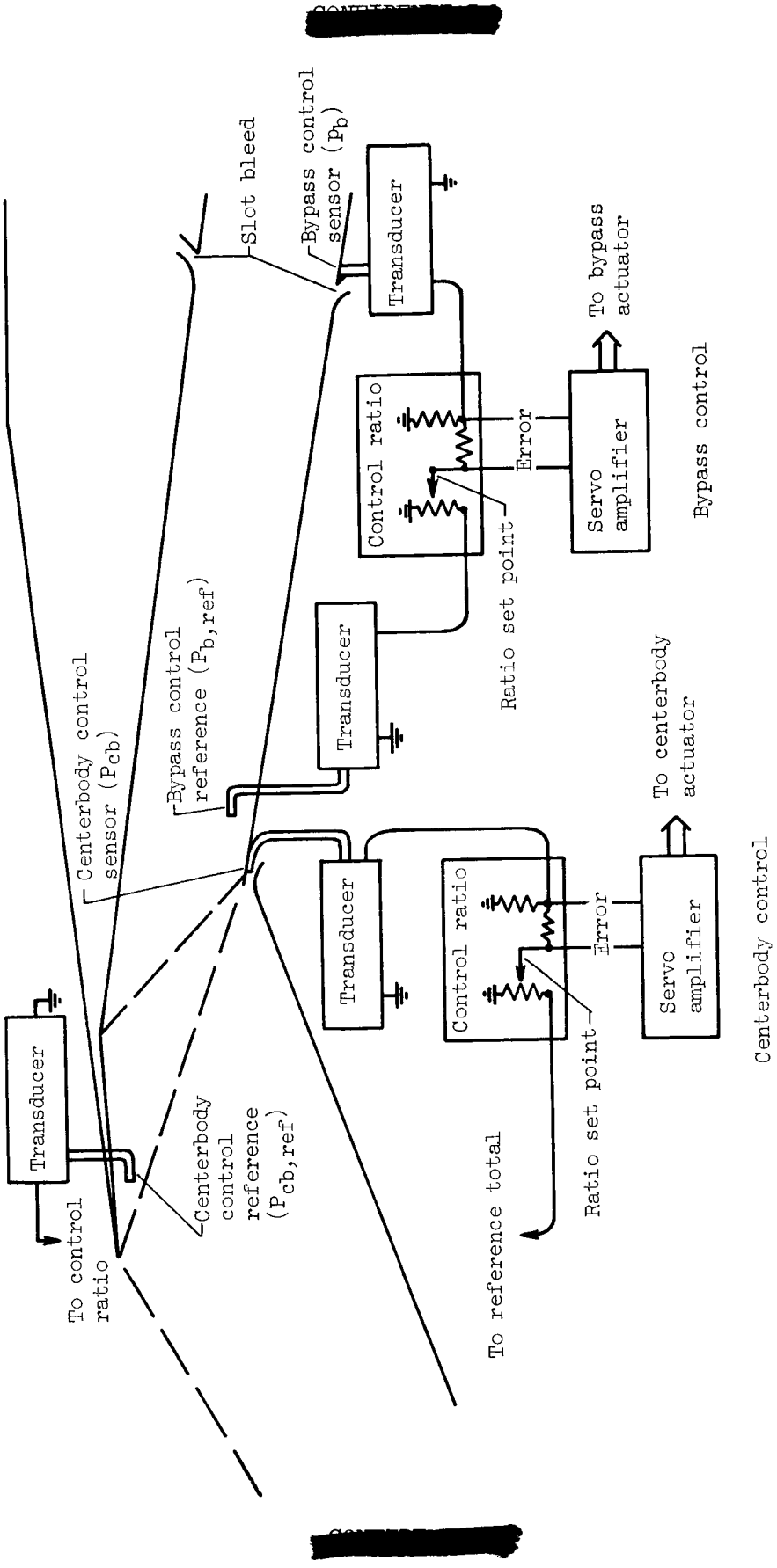

Figure 6. - Centerbody and bypass controls.

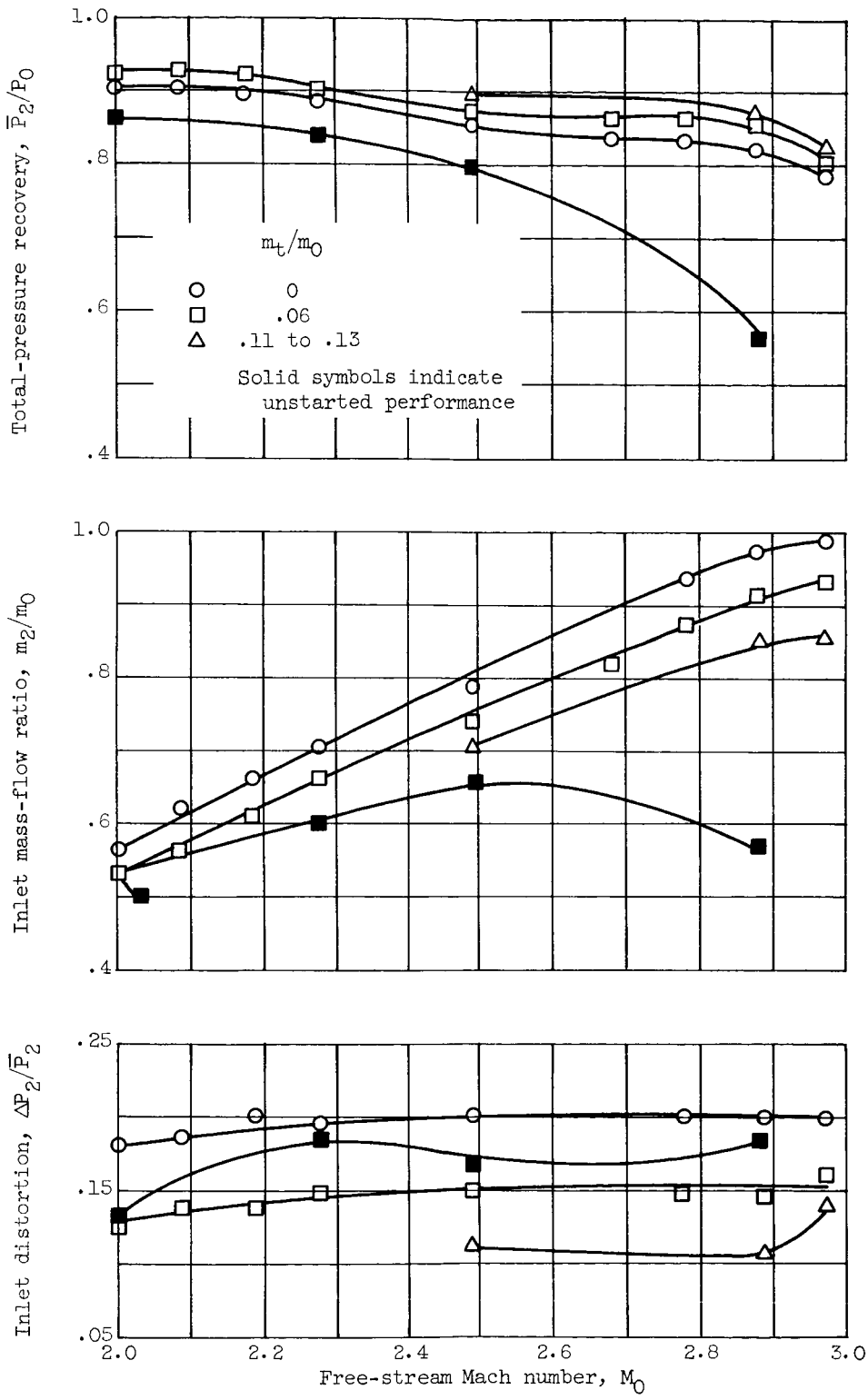

Figure 7. - Peak inlet performance from Mach 2.0 to 3.0 for different throat bleed mass-flow ratios. Centerbody shoulder bleed mass-flow ratio, 0.02.

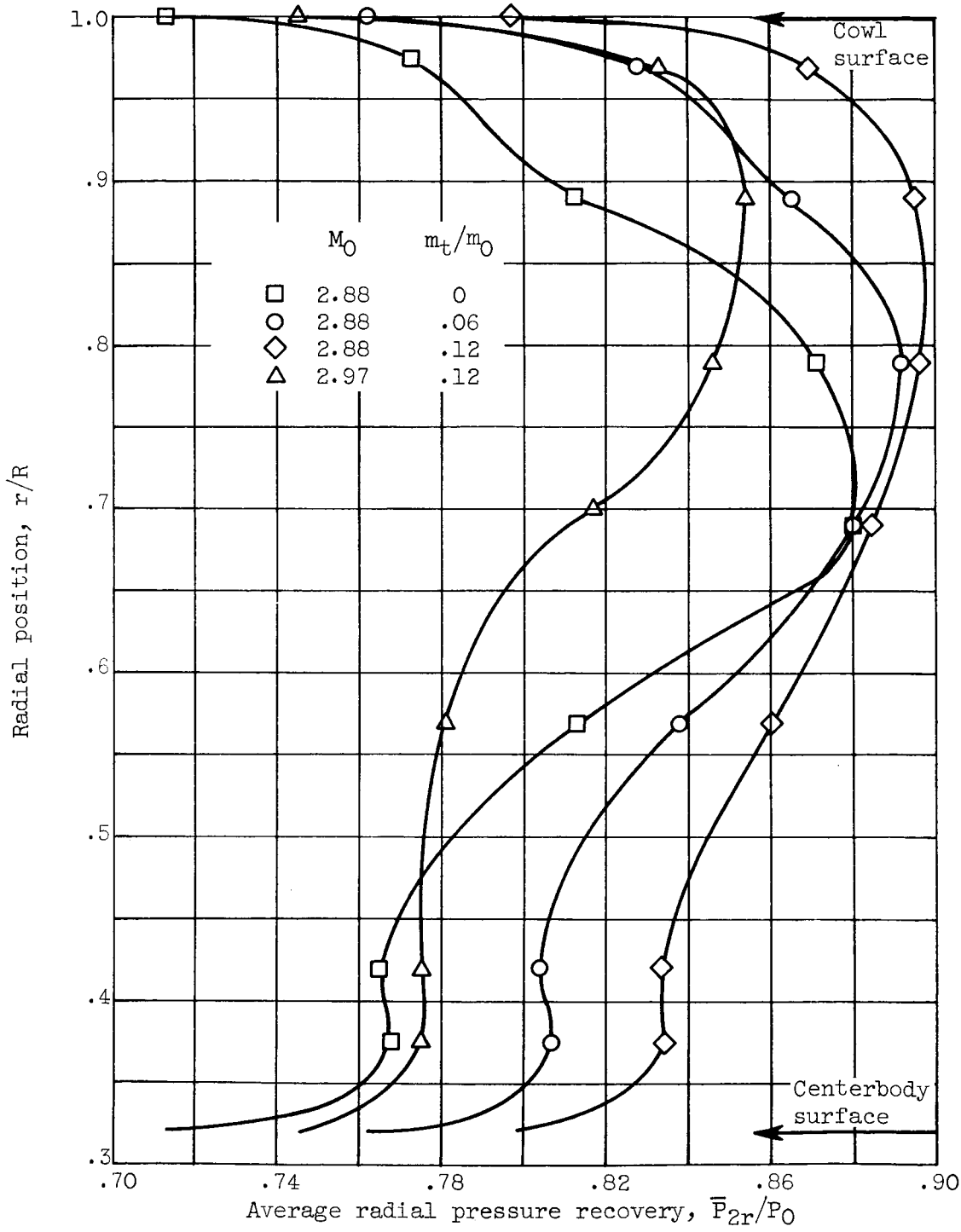

Figure 8. - Effect of bleed and Mach number on radial total-pressure distribution at engine face.

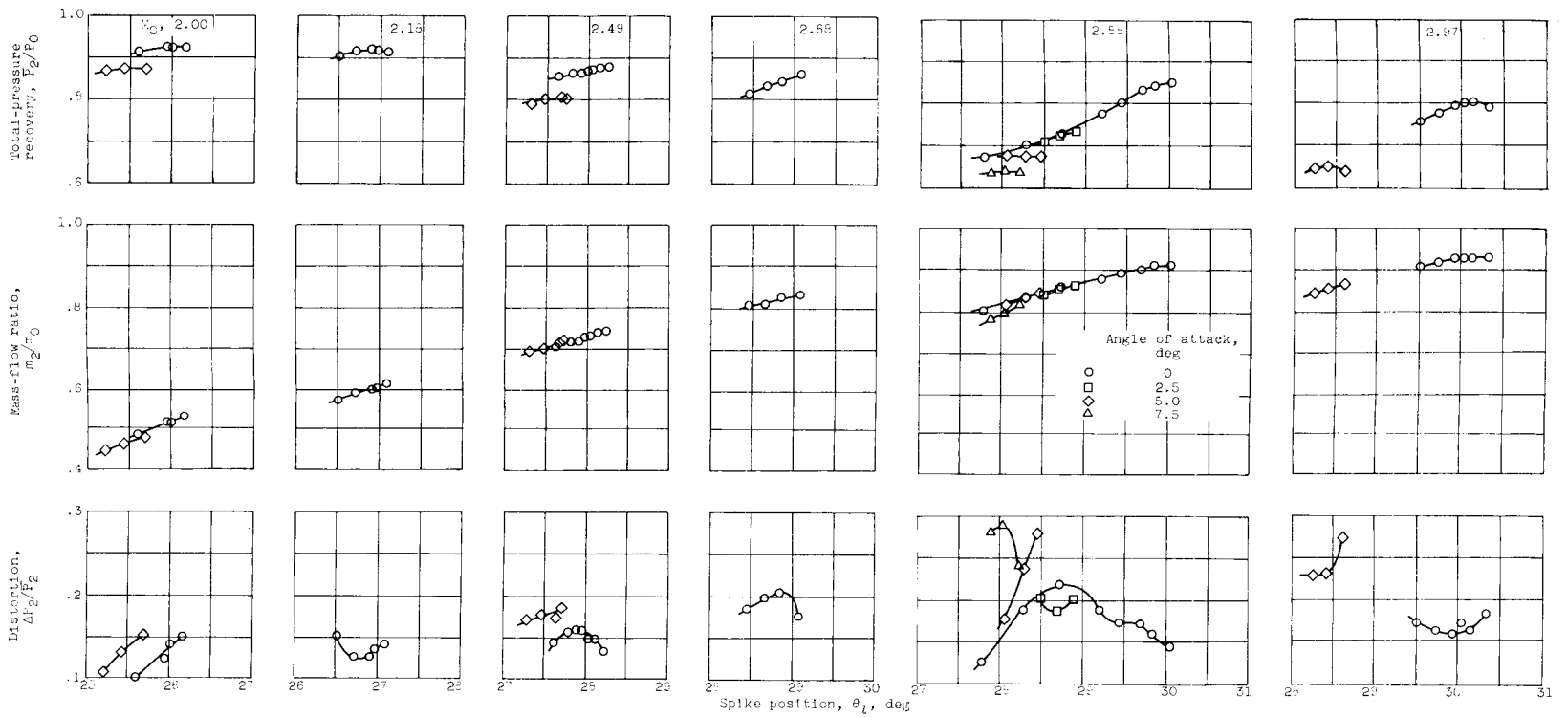

Figure 9. - General performance with maximum small slot bleed. Bypass mass flow ratio, m_b/m_0, 0; Reynolds number, 2.0×10^6 per foot; throat bleed mass-flow ratio, 0.06.

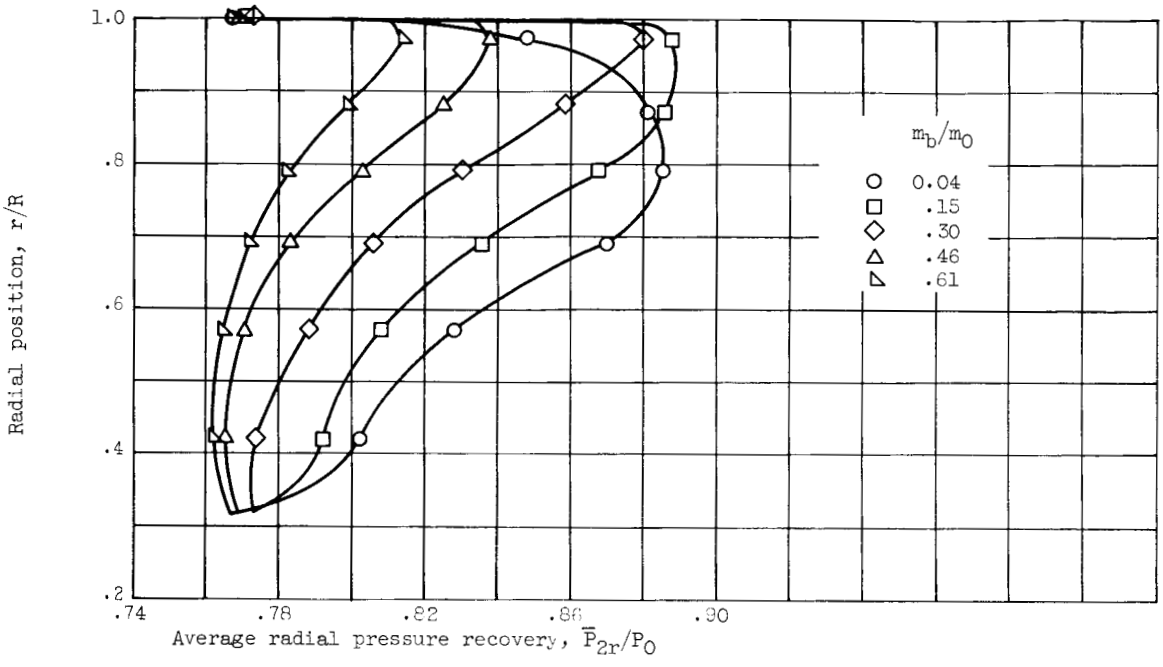

(a) Radial total-pressure distribution at engine face.

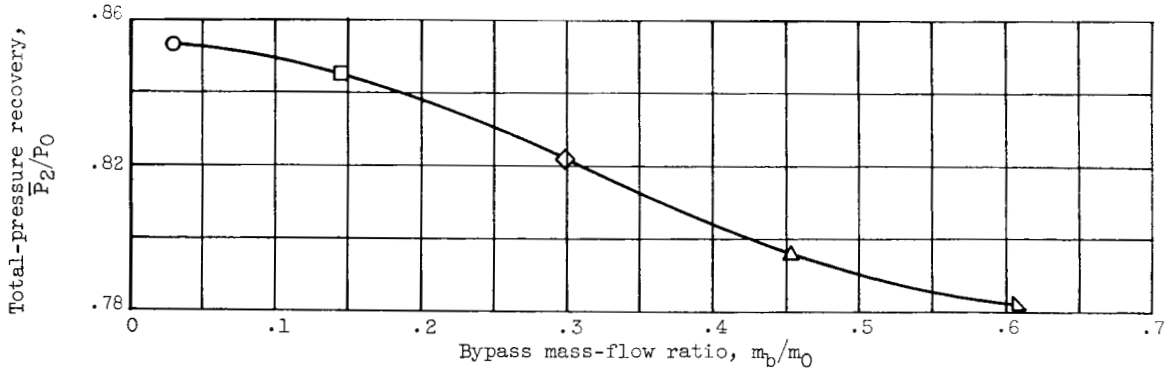

(b) Variation in recovery at engine face with bypass mass-flow change.

Figure 10. - Effect of bypass mass flow on inlet performance. Mach 2.88; angle of attack, 0°; Reynolds number, 1.98×10^6 per foot.

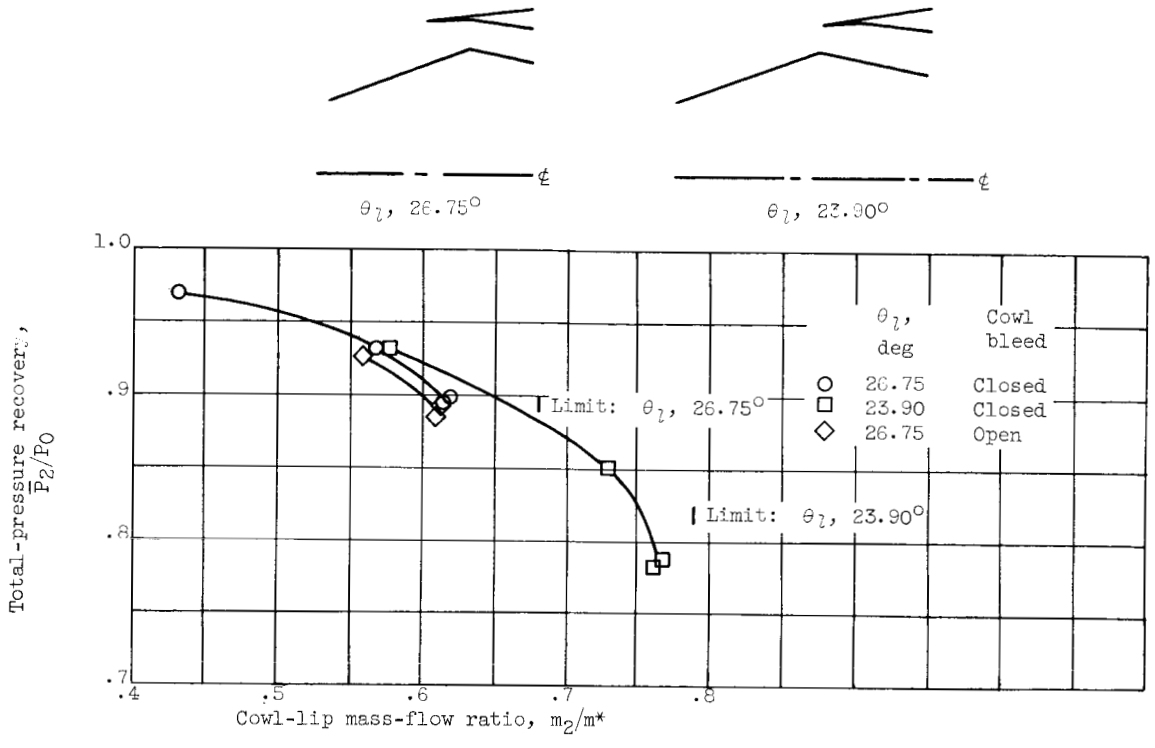

(a) Inlet recovery.

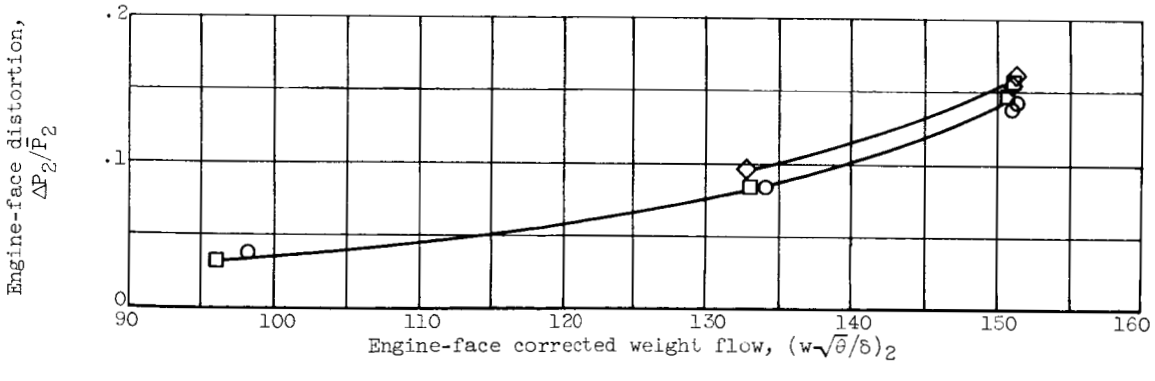

(b) Inlet distortion.

Figure 11. - Low-speed inlet performance.

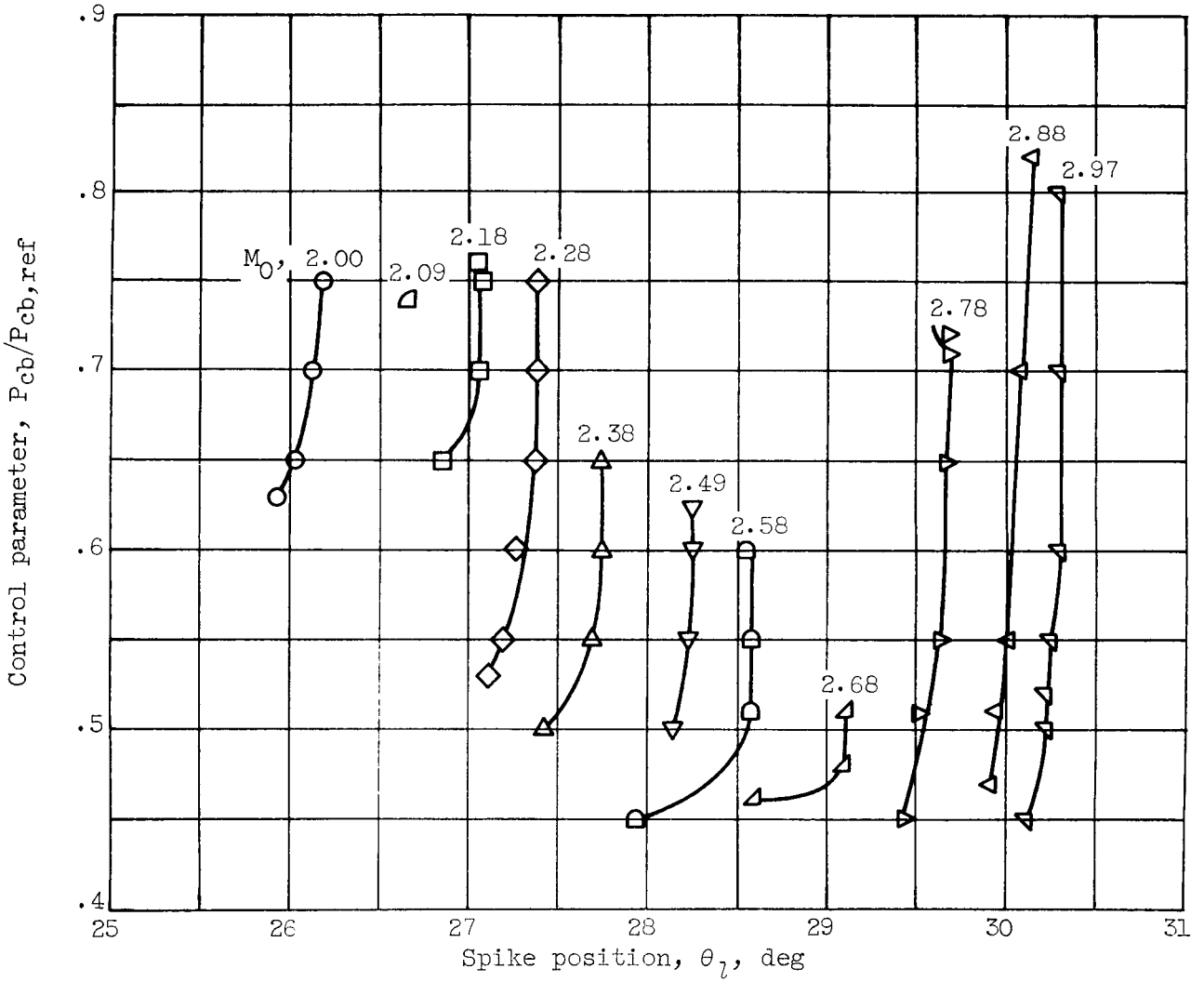

Figure 12. - Centerbody control parameter performance. Angle of attack, 0°; Reynolds number, 2.0×10^6 per foot.

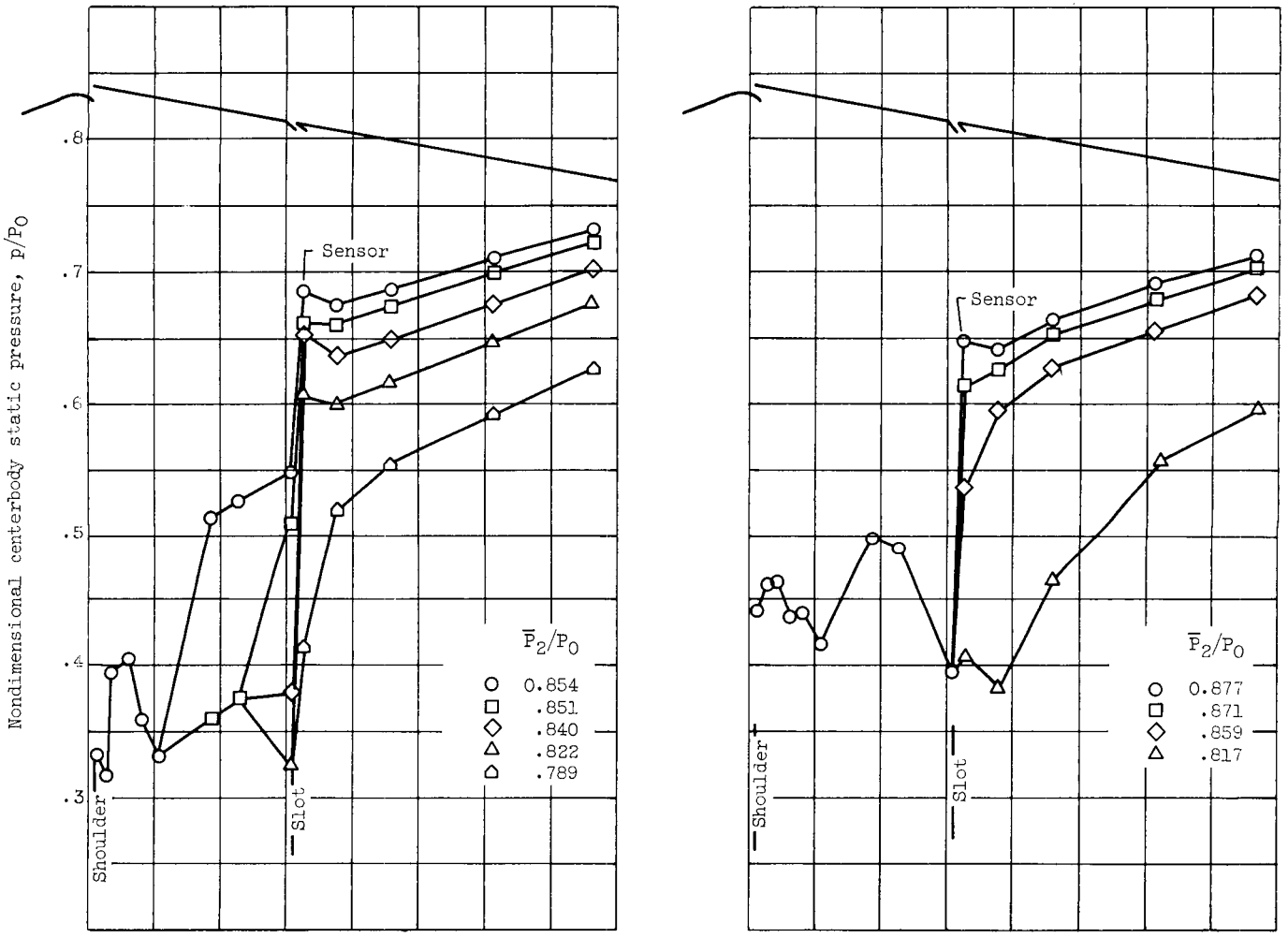

(a) Mach 2.86.

(b) Mach 2.49.

Figure 13. - Variation in static-pressure distribution on the centerbody with recovery change. Angle of attack, 0°; Reynolds number, 2.0×10^6 per foot.

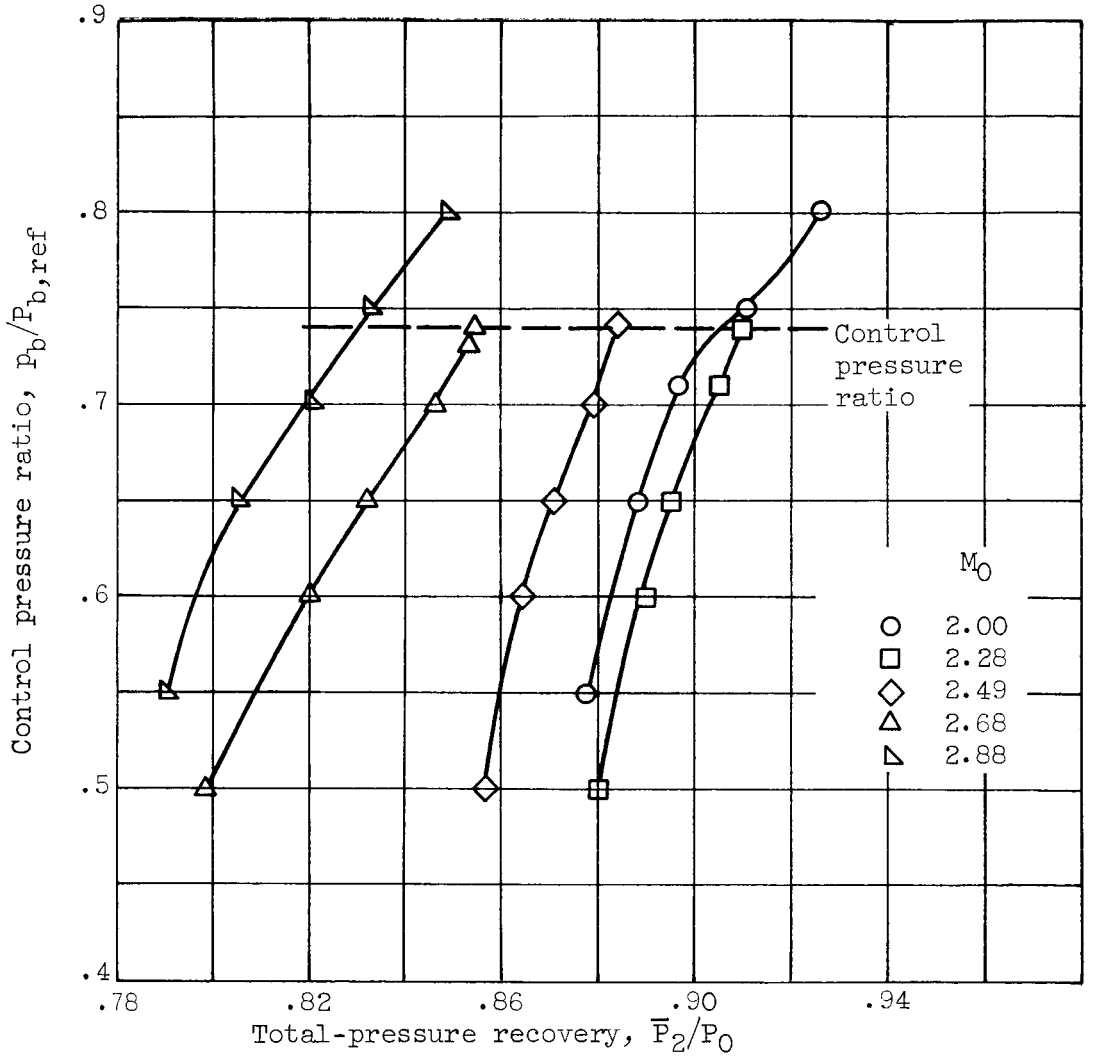

Figure 14. - Bypass control performance. Angle of attack, 0°; Reynolds number, 2.0×10^6 per foot; centerbody position, θ_l, optimum value set by centerbody control.

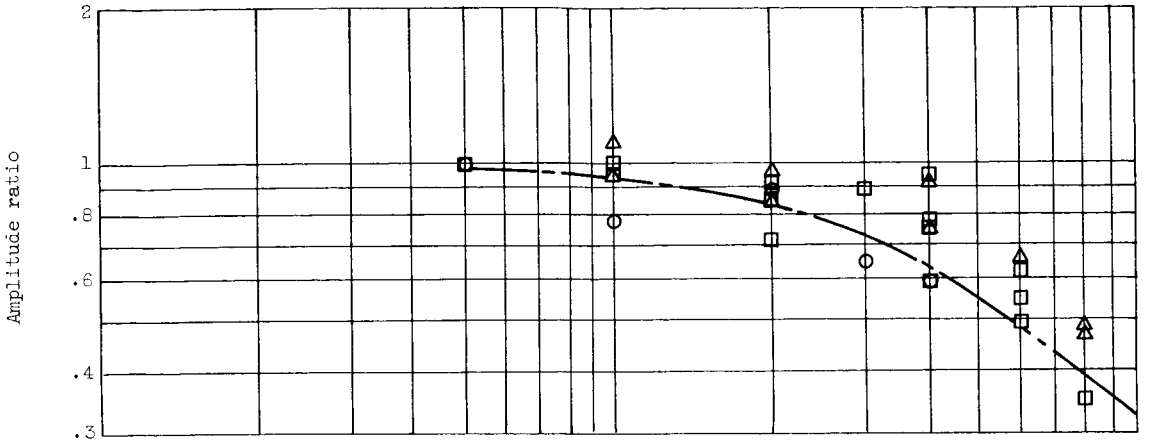

(a) Amplitude ratio from bypass static.

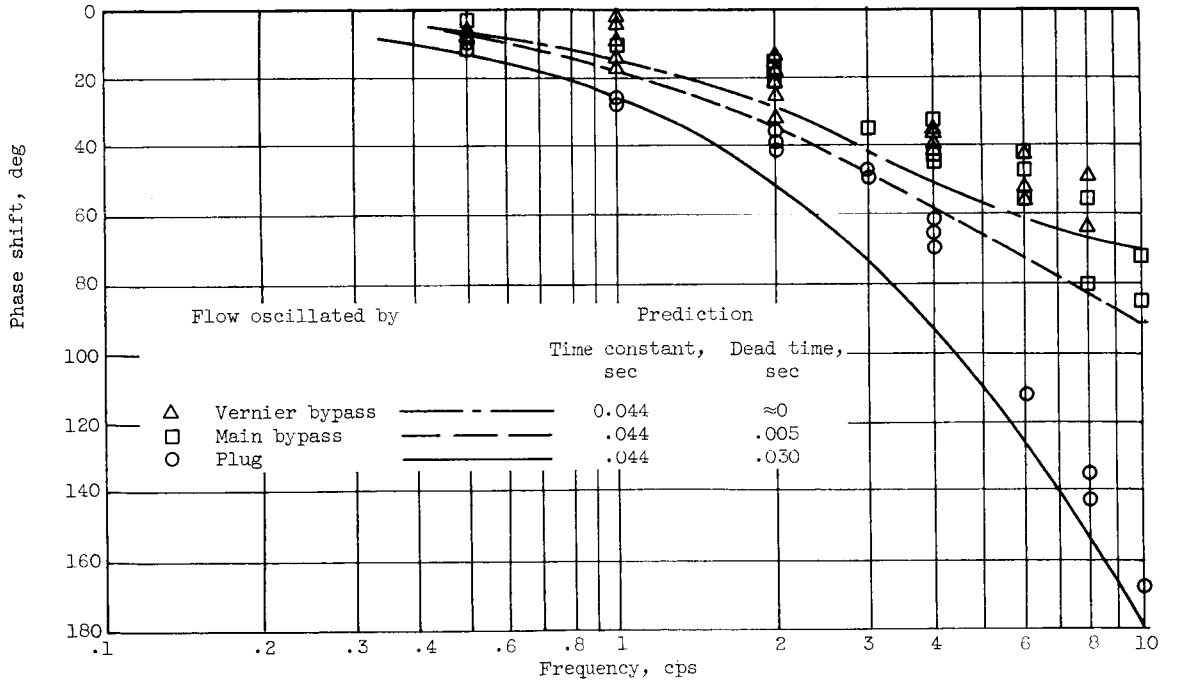

(b) Phase shift from statics near flush bleed slots.

Figure 15. - Inlet-coldpipe response of static-pressure sensor p_b to disturbances at three streamwise locations. Mach 2.88; Reynolds number, 2.0×10^6 per foot.

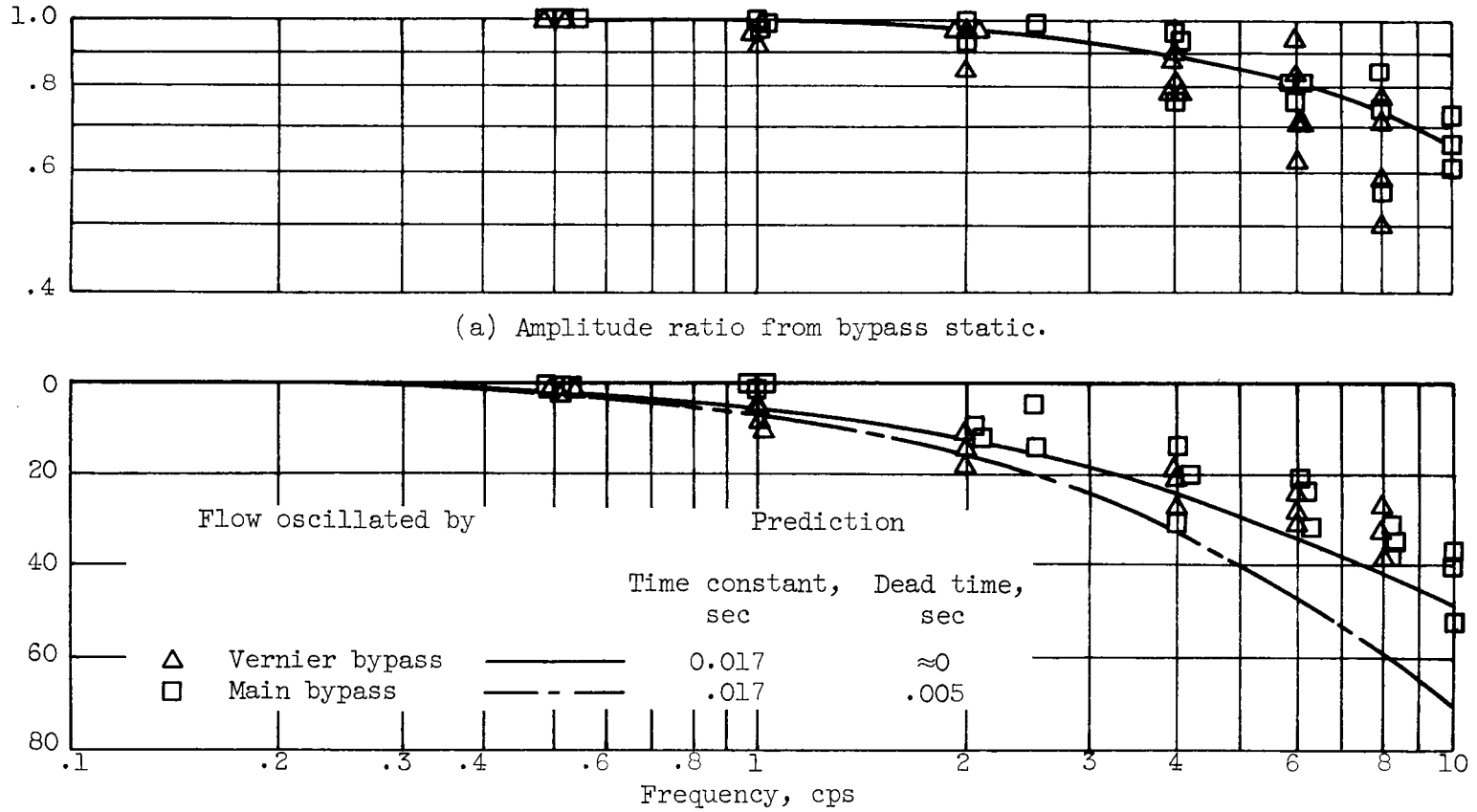

(a) Amplitude ratio from bypass static.

(b) Phase shift from statics near flush bleed slots.

Figure 16. - Inlet-engine response of static-pressure sensor p_b to disturbances at two streamwise locations. Mach 2.88; Reynolds number, 2.0×10^6 per foot.

[redacted]

NOTES: (1) Reynolds number is based on the diameter of a circle with the same area as that of the capture area of the inlet.

(2) The symbol * denotes the occurrence of buzz.

INLET BIBLIOGRAPHY SHEET

Report and facility	Description			Test parameters				Test data				Performance		Remarks
	Configuration	Number of oblique shocks	Type of boundary-layer control	Free-stream Mach number	Reynolds number × 10^{-6}	Angle of attack, deg	Angle of yaw, deg	Drag	Inlet-flow profile	Discharge-flow profile	Flow picture	Maximum total-pressure recovery	Mass-flow ratio	
CONFID. TM X-471 Lewis 10- by 10-ft Supersonic Wind Tunnel	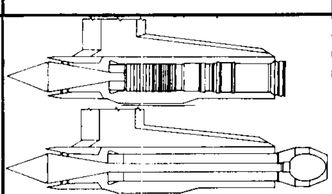	3	Flush slots	2.0 2.09 2.18 2.28 2.49 2.68 2.76 2.86 2.97	2.0	0, 5 0 0 0 0, 5 0 0 0, 2.5, 5 0, 5	0	No		Yes		0.93 .93 .92 .90 .90 .87 .87 .87 .82	0.53 .57 .61 .66 .71 .82 .87 .85 .85	Report presents inlet performance and the response of possible control pressures in the throat to sinusoidal flow oscillations at three stations in a coldpipe configuration and two stations in an engine configuration. Also, the steady-state performance of a simple inlet control is presented.
CONFID. TM X-471 Lewis 10- by 10-ft Supersonic Wind Tunnel	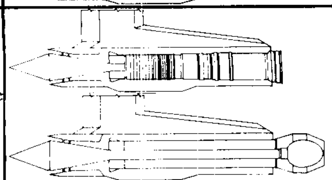	3	Flush slots	2.0 2.09 2.18 2.28 2.49 2.68 2.78 2.88 2.97	2.0	0, 5 0 0 0 0, 5 0 0 0, 2.5, 5 0, 5	0	No		Yes		0.93 .93 .92 .90 .90 .87 .87 .87 .82	0.53 .57 .61 .66 .71 .82 .87 .85 .85	Report presents inlet performance and the response of possible control pressures in the throat to sinusoidal flow oscillations at three stations in a coldpipe configuration and two stations in an engine configuration. Also, the steady-state performance of a simple inlet control is presented.
CONFID. TM X-471 Lewis 10- by 10-ft Supersonic Wind Tunnel	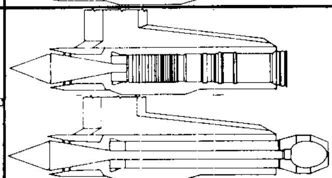	3	Flush slots	2.0 2.09 2.18 2.28 2.49 2.68 2.78 2.88 2.97	2.0	0, 5 0 0 0 0, 5 0 0 0, 2.5, 5 0, 5	0	No		Yes		0.93 .93 .92 .90 .90 .87 .87 .87 .82	0.53 .57 .61 .66 .71 .82 .87 .85 .85	Report presents inlet performance and the response of possible control pressures in the throat to sinusoidal flow oscillations at three stations in a coldpipe configuration and two stations in an engine configuration. Also, the steady-state performance of a simple inlet control is presented.
CONFID. TM X-471 Lewis 10- by 10-ft Supersonic Tunnel	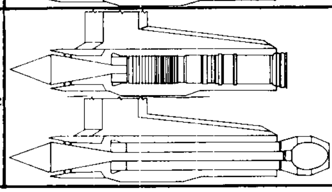	3	Flush slots	2.0 2.09 2.18 2.28 2.49 2.68 2.78 2.88 2.97	2.0	0, 5 0 0 0 0, 5 0 0 0, 2.5, 5 0, 5	0	No		Yes		0.93 .93 .92 .90 .90 .87 .87 .87 .82	0.53 .57 .61 .66 .71 .82 .87 .85 .85	Report presents inlet performance and the response of possible control pressures in the throat to sinusoidal flow oscillations at three stations in a coldpipe configuration and two stations in an engine configuration. Also, the steady-state performance of a simple inlet control is presented.

Bibliography

These strips are provided for the convenience of the reader and can be removed from this report to compile a bibliography of NASA inlet reports. This page is being added only to inlet reports.

[redacted]